HHS Public Access

Author manuscript

J Am Chem Soc. Author manuscript; available in PMC 2015 May 13.

Published in final edited form as:

J Am Chem Soc. 2013 January 9; 135(1): 174–182. doi:10.1021/ja307083b.

Functional Imaging of Legumain in Cancer Using a New Quenched Activity-Based Probe

Laura E. Edgington[†,‡], **Martijn Verdoes**[‡], **Alberto Ortega**[‡], **Nimali P. Withana**[‡], **Jiyoun Lee**[‡,⊥], **Salahuddin Syed**[‡], **Michael H. Bachmann**[§], **Galia Blum**[‡,⊥,#], and **Matthew Bogyo**[*,†,‡,∥]

[†]Cancer Biology Program, Stanford School of Medicine, 300 Pasteur Drive, Stanford, California 94305-5324, United States

[‡]Department of Pathology, Stanford School of Medicine, 300 Pasteur Drive, Stanford, California 94305-5324, United States

[§]Department of Pediatrics, Stanford School of Medicine, 300 Pasteur Drive, Stanford, California 94305-5324, United States

[∥]Department of Microbiology and Immunology, Stanford School of Medicine, 300 Pasteur Drive, Stanford, California 94305-5324, United States

Abstract

Legumain is a lysosomal cysteine protease whose biological function remains poorly defined. Legumain activity is up-regulated in most human cancers and inflammatory diseases most likely as the result of high expression in populations of activated macrophages. Within the tumor microenvironment, legumain activity is thought to promote tumorigenesis. To obtain a greater understanding of the role of legumain activity during cancer progression and inflammation, we developed an activity-based probe that becomes fluorescent only upon binding active legumain. This probe is highly selective for legumain, even in the context of whole cells and tissues, and is also a more effective label of legumain than previously reported probes. Here we present the synthesis and application of our probe to the analysis of legumain activity in primary macrophages and in two mouse models of cancer. We find that legumain activity is highly correlated with macrophage activation and furthermore that it is an ideal marker for primary tumor inflammation and early stage metastatic lesions.

[*]**Corresponding Author**: mbogyo@stanford.edu.

[⊥]**Present Address**: Department of Global Medical Science, Sungshin Women's University, Seoul 142–732, Korea.

[#]**Present Address**: Institute of Drug Research, The Hebrew University, Jerusalem, Israel 91120.

ASSOCIATED CONTENT

Supporting Information

Figure S1: LE28 Mass Spec and NMR. Figure S2: Quenching efficiency. Figure S3: In vitro LE28 labeling, related to Figure 2. Figure S4: Caspase reactivity of LE28. Figure S5: In vitro comparison of LE28 and LP-1. Figure S6: Regulation of legumain activity, related to Figure 3. Figure S7: Imaging with LP-1, related to Figure 4. This material is available free of charge via the Internet at http://pubs.acs.org.

Author Contributions

The manuscript was written through contributions of all authors. All authors have given approval to the final version of the manuscript.

The authors declare no competing financial interest.

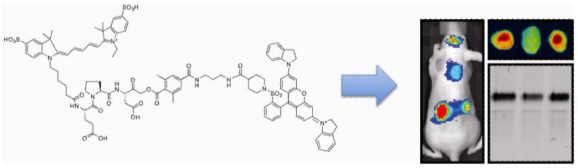

INTRODUCTION

Legumain, or asparaginyl endopeptidase, is a cysteine protease found primarily in the acidic environment of the lysosome, although in some cell types it may also be associated with the cell surface.[1,2] As its name indicates, it was first identified in legumes as a vacuolar processing enzyme with unique substrate specificity toward asparagine residues in the P1 position. Legumain is most highly expressed in the kidney, where it contributes to normal protein catabolism and renal homeostasis.[3] It also promotes extracellular matrix remodeling in proximal tubule cells through degradation of fibronectin.[4] Additionally, it, along with several members of the cysteine cathepsin family, plays important roles in immune function, where it can initiate invariant chain processing during Class II MHC antigen presentation.[5-9]

Beyond its roles in normal physiology, legumain is associated with a number of inflammatory diseases such as atherosclerosis,[4,10,11] stroke,[12] and cancer. Its expression is upregulated in the majority of solid tumors[2] and correlates with decreased survival in human patients bearing breast,[13] colorectal,[14] and ovarian[15] tumors. A number of in vitro assays have demonstrated that HEK 293 cells overexpressing legumain show increased potential for cell migration, invasion, and angiogenesis.[2] These cells also show increased metastasis from subcutaneous tumors in vivo compared to nontransfected control cells.[2] Within the tumor microenvironment, however, legumain is most highly expressed by tumor-associated macrophages (TAMs) and not by the tumor cells themselves.[16,17]

Precise roles for stromal-derived legumain have not been thoroughly defined; however, it likely contributes to the tumor-promoting inflammation associated with most malignancies.[18] One antitumor strategy involved triggering an immune response toward legumain-expressing cells with a mini-gene vaccine. This led to ablation of TAMs and subsequent reduction in tumor volume, angiogenesis, and metastasis.[17,19] Other strategies have focused on prodrugs that, when processed by legumain, release cytotoxic agents such as doxorubicin specifically in cells with high levels of active legumain.[1,2,16,20,21] These pro-drugs have been shown to have a profound impact on survival in both syngeneic and human xenograft tumor models in mice. Efficacy of these strategies illuminates important roles for legumain-expressing cells in tumor progression, invasion, and metastasis.

As with any protease, analysis of expression of legumain at the gene or protein level gives little insight into the regulation of its enzymatic activity. Legumain is synthesized as an inactive zymogen that becomes proteolytically active through an autocleavage event upon arriving in the acidic environment of the lysosome. Once active, legumain is also subject to inhibition by endogenous proteins such as the cystatins. Recently, our group reported a near-infrared fluorescent activity-based probe, LP-1, to detect legumain activity.[22] This probe contains an azaepoxide electrophile that binds specifically and irreversibly to the catalytic

thiol in the active site of legumain. Because LP-1 is not quenched, the free, unbound probe must clear before specific signals can be detected in vivo. To circumvent this problem, and thereby increase the specificity of the fluorescent signal, we describe here a “smart” legumain probe that is intrinsically quenched and becomes fluorescent only upon specific, covalent binding to legumain. This new probe shows comparable potency toward legumain in cell lysates and enhanced labeling of legumain in intact cells, organs, and tumors when compared to LP-1. We show that this reagent can be used to image legumain activity in both normal mice and in two murine models of cancer. We also use the probe to monitor the induction of legumain activity in alternatively activated bone-marrow-derived macrophages. These data provide insight into how this protease could be up-regulated in the inflammatory tumor microenvironment and provide a valuable new tool for imaging of inflammation events.

RESULTS AND DISCUSSION

Development of a Quenched Activity-Based Probe for Legumain

To generate a quenched legumain probe, we needed to utilize an electrophile that would produce a leaving group upon covalent binding with the active site cysteine. The aza-epoxide warhead in LP-1 is not suitable for such a purpose as nucleophilic attack results in opening of the epoxide ring. We turned instead to the acyloxymethyl ketone (AOMK) electrophile that we have successfully used to make quenched probes for cathepsins.[23,24] Upon binding of the enzyme to the AOMK reactive group, the *O*-acyl group is released, making it an ideal place to introduce a quenching moiety (Figure 1).

Legumain exhibits a strong preference for cleavage after asparagine residues; however, it has also been shown to bind AOMK probes containing a P1 aspartic acid.[25-27] At low pH in the lysosome, the acid side chain is protonated, thereby permitting binding in the S1 pocket of legumain. Because P1 Asn-AOMK probes are not stable over time,[27] we opted to move forward with AOMKs that contain a P1 Asp. Our previously reported probe, AB50, containing the sequence Glu-Pro-Asp-AOMK, primarily targeted caspases. However, it also demonstrated significant cross-reactivity with legumain.[28] We hypothesized that adding a bulky quenching group to AB50 would encourage uptake into the cell by macropinocytosis/endocytosis rather than direct entry into the cytoplasm. Sequestration of the probe in the endosomal pathway would increase access to legumain and limit interaction with caspases, thereby producing a legumain-selective quenched probe.

We first compared fluorescence emission of increasing concentrations of both AB50 and LE28 and found LE28 to be highly quenched (Figure S2, Supporting Information). To test the capacity for LE28 to bind legumain, we first used cell extracts prepared from mouse macrophages (RAW 264.7 cells) lysed in citrate buffer (pH 4.5). (To verify equal loading in this and subsequent experiments, we have included data from our BCA protein quantification assays. Protein concentration was measured for each experiment, and uniform amounts of protein were used for each sample within the same gel (Figure S3, Supporting Information).) We incubated these extracts with increasing concentrations of LE28, and then proteins were resolved by SDS-PAGE followed by scanning for Cy5 fluorescence. We observed labeling of a single legumain species at 36 kDa (Figure 2a). This band was

detectable at probe concentrations as low as 100 pM with an EC50 ~10 nM and saturation above 50 nM. To confirm that the labeled species was indeed legumain, we performed an immunoprecipitation assay on probe-labeled lysates with a legumain-specific polyclonal antibody (Figure 2b). To verify that LE28 was activity-dependent, we preincubated RAW cell lysates with recombinant cystatin C, a naturally expressed legumain inhibitor, followed by addition of LE28. We observed dose-dependent competition of legumain labeling by LE28 (Figure S4a, Supporting Information). Cystatin C N39A, a mutant lacking the residue critical for legumain binding, however, was unable to block labeling.

Next, we examined the ability of LE28 to label legumain in intact RAW cells. As in lysates, we observed exclusive labeling of legumain at all concentrations tested (Figure 2c). We also performed a labeling time course in intact cells. Legumain activity could be detected as little as 30 min after probe addition and was saturated after two hours (Figure 2d). We also performed identical experiments in COLO205 colorectal cancer cells. While the potency of LE28 was similar in both cell lines (Figure S4b, Supporting Information), we found that saturation of legumain labeling in COLO205 cells did not occur until four hours after probe addition (Figure S4c, Supporting Information). The more rapid uptake by macrophages supports our hypothesis that the probe enters cells by endocytosis or macropinocytosis.

Next, we examined the LE28-labeled RAW cells by microscopy. We observed a punctate staining pattern consistent with lysosomal accumulation. As anticipated, LE28 staining colocalized with Lysotracker, confirming lysosomal distribution (Figure 2e). To show that the fluorescent signal was specific to legumain, we also treated RAW cells with a legumain-specific inhibitor, LI-1,[22] prior to the addition of LE28. Compared to a control that was pretreated with a DMSO vehicle, the LI-1 treated cells showed dramatically less signal (Figure 2f). To verify that this was due to legumain inhibition, we also analyzed cells treated in parallel by fluorescent SDS-PAGE. Indeed, nearly all of the LE28 labeling was blocked upon pretreatment with LI-1 (Figure 2g).

LE28 Reactivity toward Caspases

In RAW cells, the quenched probe LE28 exhibited specific labeling of legumain. Since its structure was designed based on our nonquenched caspase probe, AB50, we wondered whether it retained reactivity toward caspases. We used an in vitro model of apoptosis in which COLO205 cells were stimulated with anti-DR5, a monoclonal antibody that initiates the extrinsic apoptosis pathway.[28-30] As we observed previously, AB50 labeled caspases and legumain at similar levels in intact cells (Figure S5a, Supporting Information). LE28, however, showed virtually no detectable caspase labeling and dramatically increased legumain labeling. When labeling was carried out in apoptotic lysates at neutral pH, both probes labeled caspases; however, LE28 was far less potent (Figure S5b, Supporting Information). In acidic pH, both probes labeled multiple legumain bands (Figure S5c, Supporting Information). These bands were confirmed to be legumain by immunoprecipation with a legumain-specific antibody (Figure S5d, Supporting Information). Taken together, these data indicate that the bulky quenching group on LE28 effectively reduces the probe's affinity for caspases and sequesters it within the endocytic pathway, where it binds exclusively to legumain.

In Vitro Comparison of LE28 and LP-1

Next we wanted to compare the efficacy of LE28 with that of the aza-asparagine epoxide probe, LP-1, which is the current gold standard for detecting legumain activity in vitro and in vivo.[22] Labeling was comparable with both probes in RAW cell extracts (pH 4.5) where LP-1 showed slightly increased potency compared to the LE28 probe (Figure S6a, Supporting Information). In intact cells, on the other hand, LE28 labeled more legumain at 1 μM than LP-1 (Figure S6b, Supporting Information), perhaps due to increased uptake of LE28 into the lysosomes compared to the less bulky LP-1.

LE28 contains a P1 aspartic acid, which requires protonation to initiate legumain binding, while LP-1 has a P1 asparagine. To examine the pH dependence of both probes, we lysed RAW cells in citrate buffer at varying pH, followed by labeling with either LE28 or LP-1 (Figure S6c, Supporting Information). We found that LP-1 labeled legumain equally well up to pH 6 and then dropped off sharply at neutral pH, consistent with the reported pH dependence of legumain.[31] As expected, LE28 labeling decreased markedly above pH 5 due to the need for protonation of the aspartate side chain, and no labeling was observed at neutral pH.

Regulation of Legumain Activity

Little is known about how legumain expression and activity is regulated in the tumor microenvironment. One study reported that legumain expression is upregulated in RAW cells exposed to the cytokines IL-4, IL-10, or IL-13, which differentiate macrophages to the M2 phenotype.[17] We were unable to recapitulate these results in our laboratory and found that RAW cells basally express high legumain levels. To further investigate legumain activity in macrophages, we turned to freshly differentiated macrophages isolated from murine bone marrow. Primary macrophages were stimulated for 96 h followed by labeling with LE28.

IL-4 treatment resulted in an increase of both expression and activity of legumain compared to nonstimulated controls (Figure 3a,b). Conversely, IL-10 treatment did not affect legumain levels. This was surprising given that in dendritic cells IL-10 has been shown to down-regulate expression of cystatin C, an endogenous legumain inhibitor.[32] When we treated macrophages with both IL-4 and IL-10 simultaneously, we observed considerable up-regulation of three species, which were confirmed to be processed forms of legumain by immune precipitation (Figure S7a, Supporting Information). We considered the possibility that the increase in legumain activity that we observed may have been due to increased uptake of LE28 by activated macrophages that have an increased potential for endocytosis of extracellular material. Therefore, we also performed a parallel experiment in which macrophages were lysed post cytokine treatment and then labeled with LE28 (Figure S7b, Supporting Information). The same activation trend was observed, confirming an up-regulation of legumain activity in response to cytokine treatment. In lysates, however, the 24 kDa protein was not observed, suggesting that it may be perturbed by the lysis conditions.

We also examined the kinetics of legumain up-regulation in response to IL-4/-10 stimulation. A substantial increase was detected as early as 24 h after exposure, and activity/

expression continued to rise throughout the time course (Figure 3c,d). Appearance of the 24 kDa legumain band occurred only after 72 h, suggesting regulated processing as macrophages become more active. When lysates were labeled, we observed the same time-dependent increase in legumain activity as found in intact cells (Figure S7c, Supporting Information).

Next we compared the legumain activity of the 4T1 breast tumor cell with that of primary macrophages (Figure 3e). When we cocultured an equal number of tumor cells and macrophages, we saw a sharp increase in legumain activity. This suggests that factors such as IL-4 and IL-10 (and most certainly others) released by tumor cells are able to significantly induce the expression and activation of legumain in macrophages, though additional experiments are needed to confirm this. Lysates prepared from xenografted tumors also showed elevated levels of legumain activity compared to the parental 4T1 line, suggesting macrophage infiltration and legumain regulation within the tumor microenvironment. We also performed similar experiments with two other cancer cell lines. Legumain activation in COLO205 colon cancer cells followed the same trend as 4T1 cells (Figure S7d, Supporting Information). However, HCT116 colon cancer cells showed very little up-regulation both in coculture and in vivo (Figure S6e, Supporting Information).

In Vivo Imaging with LE28

While LE28 and LP-1 were both effective activity-based probes for legumain in vitro, we anticipated that the real advantage of LE28 would be for optical imaging. Because LE28 is quenched, it should have dramatically improved in vivo properties since there is no need for clearance of the unbound probe to obtain image contrast. We therefore examined probe clearance by optical imaging in healthy nude mice. LE28 was injected by the tail vein following imaging of Cy5 fluorescence over time using the IVIS 100 system (Figure 4a). LE28 produced low fluorescence at early time points. A specific signal in the kidney became detectable after about one hour and continued to increase over time. Injection of LP-1, on the other hand, resulted in whole body fluorescence at early time points, and after one hour, most of the fluorescent signal had disappeared (Figure S8a, Supporting Information).

After eight hours, we collected the major organs from mice injected with each probe and performed a biochemical analysis. For both probes, the highest labeling was observed in the kidney and to a lesser extent the liver (Figure 4b and Figure S8b, Supporting Information). In fact, LE28 labeling in the kidneys was so high that it was possible to visualize the probe signal using the noninvasive fluorescence imaging methods, which are limited by poor penetration depth. Low levels of signal were also detected in the spleen, intestine, pancreas, and heart, but not in the lungs or brain. The distribution of labeling in the organs was largely consistent with the total legumain levels as detected by Western blot (Figure 4c). However, the Western blot shows higher levels of legumain in the spleen than detected by LE28 or LP-1. This may reflect inhibition of legumain in the spleen or poor probe delivery to this organ. While the labeling patterns for both probes were very similar, the intensity of the LE28 signal was more than five times brighter than LP-1. We attribute this difference to the increased half-life of LE28 in combination with the enhanced cellular uptake that we observed in vitro. Furthermore, analysis of tissues after 28 h probe circulation revealed

nearly identical levels of probe labeling, indicating that LE28-bound legumain is sustained over time (Figure S8c, Supporting Information). The most mature form of legumain was previously reported to be 36 kDa. In the kidney and liver, labeled proteins with molecular weights lower than 36 were confirmed to be processed forms of legumain, as shown by immunoprecipitation with a legumain-specific antibody (Figure S8d,e, Supporting Information).

We also wanted to assess the ability of LE28 to detect legumain in tumors by noninvasive imaging. To this end, we used a simple xenograft model using HCT-116 human colorectal carcinoma cells. We injected tumor-bearing mice with LE28 and monitored whole body fluorescence over the course of 28 h. The LE28 signal could be detected around the periphery of the tumors in as early as 30 min with gradual penetration throughout the tumor over time (Figure 4d). Maximal contrast between tumor and normal tissue was achieved after seven hours, and the signal remained constant up to 28 h. Importantly, ex vivo fluorescence correlated with levels of legumain labeling by SDS-PAGE (Figure 4e). In the same experiment, we also performed a direct comparison of LE28 to the nonquenched probe, LP-1 (Figure S9, Supporting Information). LE28 showed much brighter tumor signal, which persisted for longer than that of LP-1. LE28 also produced better contrast of the tumor over the surrounding normal tissue (Figure S9a–c, Supporting Information). Futhermore, the ex vivo fluorescence produced by LE28 was strikingly brighter than LP-1, corresponding to dramatically increased labeling of legumain as assessed by SDS-PAGE (Figure S9d, Supporting Information).

Imaging Legumain Activity in a Syngeneic Tumor Model

Legumain is highly expressed in macrophages and plays roles in immune function. Infiltration of immune cells into the tumor has been shown to be a hallmark of tumorigenesis and contributes to the smoldering inflammation characteristic of the tumor microenvironment. The nude mice used in the previous study lack a complete immune system; therefore, we wanted to test LE28 in a more physiologically relevant model. We turned to a syngeneic model using immunocompetent Balb/c mice. 4T1 cells derived from a spontaneous mouse mammary tumor were injected by tail vein to simulate metastasis. Since the cells were engineered to express luciferase, tumor progression could be monitored by bioluminescence imaging. Once tumors were established, we injected LE28. Six hours later, we injected luciferin and then performed bioluminescence and fluorescence imaging and biochemical analysis of excised tissues (Figure 5a). The majority of mice developed nodules in the lung. We found that even the smallest nodules that we could detect by luciferase were positive for Cy5 fluorescence and thus legumain activity (Figure 5b). No signal was detected in naïve lungs. As the tumor burden increased, we saw increased levels of fluorescence, which largely colocalized with luciferase activity but also spread to the surrounding normal tissue. We believe this is due to the fact that LE28 provides a broad measure of inflammation of the lung, while the luciferase signal remains confined to tumor tissues. Solid tumors also appeared throughout the peritoneum, and these tissues were also positive for the LE28 probe signal.

When we analyzed whole lung lysates by SDS-PAGE, we found that legumain levels were increased in tissues with high tumor burden compared to normal lungs and those with few tumors. We were surprised to see labeling of additional protein bands in the lungs with high tumor burden (Figure 5c). These labeled proteins were consistent with the sizes of the lysosomal cysteine cathepsins. Their identity was confirmed by immunoprecipitation with cathepsin-specific antibodies (not shown). When we dissected out individual lung tumors, however, labeled cathepsins were not observed (Figure 5d). This indicates that cathepsin labeling may result from high levels of these proteases due to inflammation in the surrounding tissues. Solid tumors isolated from other parts of the body produced considerably higher levels of legumain activity than the lung tumors, indicating that the metastatic niche may be important for legumain regulation.

CONCLUSIONS

In this study, we present a newly designed activity-based probe for the lysosomal protease legumain. We found that the main advantage of LE28 over previously reported legumain probes is that it is fluorescently quenched and therefore acts as a smart probe that can be used for real-time imaging of legumain activity. Because no fluorescent signal is produced until the probe binds active legumain, the background signal is dramatically reduced, and the need for clearance of the free probe is eliminated. Furthermore, enhanced signal-to-noise ratios makes LE28 ideal for microscopy experiments and in vivo imaging. An added benefit of the large, bulky quenching group is that it appears to enhance uptake of the probe into the lysosomal compartments of cells. As a result, LE28 provides brighter legumain signal in vivo compared to nonquenched probes such as LP-1.

We used LE28 to image legumain activity in normal tissues in naïve mice and in inflammation associated with xenografted tumors and metastases in a syngeneic model. In addition to kidney and liver, where legumain is constitutively active, we observed an accumulation of fluorescent signal in tumors. Contrary to some reports that legumain is only expressed in macrophages within the tumor microenvironment,[16] in vitro, we clearly detect legumain in primary macrophages, and its activity increases upon exposure to inflammatory cytokines or tumor cells. We also detect varying levels of activity in several tumor cell lines in vitro.

Studies using legumain-activated prodrugs highlight the importance of legumain-expressing cells during tumor progression.[1,2,16,20,21] However, precise roles for legumain activity within both tumor and stroma have yet to be carefully delineated. It is also not clear whether blocking the activity of legumain could have a therapeutic effect in a number of conditions involving inflammation. LE28 will likely have great value in future efforts to assess the potential of this protease as a drug target in cancer and diseases involving increased inflammation.

MATERIALS AND METHODS

Probe Synthesis

The synthesis of LE28 is outlined in Scheme 1 and described in detail in the Supporting Information (Figure S1).

Lysate Labeling

Cells were seeded in six-well plates (typically 1.5×10^6/well) 24 h prior to harvest. Cells were then washed once with PBS, scraped, and pelleted. Cells were then lysed in acidic buffer (50 mM sodium citrate [pH 4.5], 0.1% CHAPS, 1% NP-40, and 4 mM DTT), snap-frozen in liquid N_2, and centrifuged at 4 °C for ten minutes. Supernatants were collected, and protein concentration was determined using a BCA kit. An amount of 40 μg of total protein was then aliquotted, followed by addition of the indicated probe from a 100× DMSO stock solution, yielding a final DMSO concentration of 1%. Samples were incubated for 30 min at 37 °C and then solubilized with 4× sample buffer. Proteins were resolved by 15% SDS-PAGE and scanned using a Typhoon flatbed laser scanner (excitation 633 nm/emission 670 nm). For the pH dependence assay, citrate buffer was adjusted to the indicated pH just prior to lysis.

Intact Cell Labeling

Cells were seeded as above 24 h prior to labeling. Media were replaced, and a probe was added from a 1000× DMSO stock solution, yielding a final DMSO concentration of 0.1%. Cells were incubated for 1 h at 37 °C unless otherwise noted, washed once with PBS, scraped, and pelleted. Cells were then lysed in hypotonic lysis buffer (50 mM PIPES [pH 7.4], 10 mM KCl, 5 mM $MgCl_2$, 2 mM EDTA, 4 mM DTT, and 1% NP-40), snap-frozen, and centrifuged at 4 °C. Supernatants were then solubilized with 4× sample buffer, and 40 μg of total protein was analyzed by SDS-PAGE as above.

Tissue Labeling

Tissues were sonicated in muscle lysis buffer (1% Triton X-100, 0.1% SDS, 0.5% sodium deoxycholate, 4 mM DTT, PBS [pH 7.4]) and analyzed as above.

Assessing Caspase Cross-Reactivity

COLO205 human colon cancer cells were plated in six-well dishes 24 h prior to treatment. Medium was refreshed, and anti-DR5 (20 μg/mL) was added for 4 h followed by hypotonic lysis as above. For intact labeling experiments, probes were added at the time of anti-DR5 treatment. For lysate labeling, probes were added to 50 μg of apoptotic lysate for one hour. Samples were analyzed by SDS-PAGE as above.

Microscopy

RAW cells were seeded at a density of 100 000 cells in an eight-well coverslip chamber (Lab-Tek). Twenty-four hours later, cells were treated with either a DMSO or 1 μM probe for five hours. For the last 30 min, Lysotracker-green (100 nM) was added to the cells. Cells were then washed three times with PBS, and phenol red-free complete medium was added.

Cells were imaged live at 40× using a Zeiss Axiovert 200 M confocal microscope in both Cy5 and FITC channels. For the competition experiment, cells were pretreated with LI-1 or DMSO for one hour, followed by addition of 1 μM LE28 for 5 h, followed by epifluorescent imaging with the same microscope.

Bone-Marrow-Derived Macrophages

Tibias and femurs were flushed with DMEM, and red blood cells were eliminated with PharmLyse (BD). The remaining cells were plated in DMEM containing 10 ng/mL of M-CSF for five days to promote macrophage differentiation. On the fifth day, cells were plated in six-well dishes at a density of 1×10^6 cells/well. IL-4, IL-10, or both (10 ng/mL) were added to the cells for the indicated number of days. Alternatively, macrophages were cocultured at a one-to-one ratio for four days. At the end of the experiment, cells were either labeled with 1 μM LE28 or lysed in citrate buffer, pH 4.5, and then labeled, followed by SDS-PAGE analysis as above.

Western bBotting

Western blots were performed according to standard procedure. Sheep antimouse legumain affinity purified polyclonal antibody was purchased from R&D Systems (AF2058) and used at 1:1000 in 5% milk/PBS-T overnight at 4 °C. Donkey antisheep-HRP secondary was used at 1:3000 for one hour at RT.

Immunoprecipitation

An amount of 100 μg of probe-labeled protein was diluted into 500 μL of RIPA buffer (PBS [pH 7.4], 1 mM EDTA, 0.5% NP-40) along with 5 μL of sheep antimouse legumain antibody. Samples were incubated on ice for 10 min followed by addition of 40 μL of slurry of prewashed Protein A/G agarose beads (Santa Cruz). Samples were agitated overnight at 4 °C. The supernatant was removed and precipitated with acetone followed by freezing for two hours, centrifugation at high speed, and resuspension in 1× sample buffer. The beads were washed four times with RIPA buffer and once with 0.9% NaCl and then boiled in 2× sample buffer. Input, pulldown, and supernatant samples were analyzed by SDS-PAGE as above.

Assessing Legumain Activity in Healthy Mice

All animal experiments were performed according to specific guidelines approved by the Stanford Administrative Panel on Laboratory Animal Care. Eight-week-old nude mice (Charles Rivers) were injected with LE28 (20 nmol in 20% DMSO/PBS, ~2 mg/kg) by tail vein. Mice were anesthetized with isofluorane and then imaged at the indicated time points using an IVIS 100 system. Tissues were removed and analyzed by SDS-PAGE as above.

Xenograft Tumor Model

Six-week-old, female nude mice were purchased from Charles Rivers. HCT-116 human colorectal carcinoma cells (3×10^6 in 30 μL of 0.5% BSA/PBS, ATTC) were injected subcutaneously on their backs and permitted to grow for eight days. The indicated probe was injected at a dose of 20 nmol in 20% DMSO/PBS and imaged using the IVIS 100 system at

the indicated time points. Tumors were then removed, imaged ex vivo using an FMT system, and analyzed by SDS-PAGE as described above.

Syngeneic Experimental Lung Metastasis Model

Six-week-old Balb/c mice were purchased from Jackson Laboratories. One hundred thousand 4T1 mouse mammary cancer cells expressing both GFP and luciferase were injected by tail vein. Tumor growth was monitored using the IVIS 100 system by bioluminescence imaging 10 min after intraperitoneal injection of D-luciferin (150 mg/kg in PBS). Once tumors were established, mice were injected with probes at a dose of 20 nmol in 20% DMSO/PBS. Six hours later, mice were injected with D-luciferin as above, and tissues were imaged for both bioluminescence and fluorescence using the IVIS 100 system. Lysates were prepared from whole lungs for SDS-PAGE analysis as described above.

Supplementary Material

Refer to Web version on PubMed Central for supplementary material.

ACKNOWLEDGMENTS

This work was supported by a grant from the National Insittutes of Health (R01 EB005011 to MB). The authors would like to thank M. Abrahamson for the kind gift of recombinant Cystatin C mutants. We also thank T. Doyle at the Stanford Small Animal Facility for assistance with the optical imaging studies. Lastly, we thank S. Lynch at the Stanford NMR Facility and A. Chien and T. McLaughlin at the Stanford Mass Spec Facility for their assistance with detailed compound characterization.

REFERENCES

(1). Liu C, Sun C, Huang H, Janda K, Edgington T. Cancer Res. 2003; 63:2957. [PubMed: 12782603]

(2). Liu Y, Bajjuri KM, Liu C, Sinha SC. Mol. Pharm. 2012; 9:168. [PubMed: 22044266]

(3). Miller G, Matthews SP, Reinheckel T, Fleming S, Watts C. FASEB J. 2011; 25:1606. [PubMed: 21292981]

(4). Morita Y, Araki H, Sugimoto T, Takeuchi K, Yamane T, Maeda T, Yamamoto Y, Nishi K, Asano M, Shirahama-Noda K, Nishimura M, Uzu T, Hara-Nishimura I, Koya D, Kashiwagi A, Ohkubo I. FEBS Lett. 2007; 581:1417. [PubMed: 17350006]

(5). Maehr R, Hang HC, Mintern JD, Kim YM, Cuvillier A, Nishimura M, Yamada K, Shirahama-Noda K, Hara-Nishimura I, Ploegh HL. J. Immunol. 2005; 174:7066. [PubMed: 15905550]

(6). Shirahama-Noda K, Yamamoto A, Sugihara K, Hashimoto N, Asano M, Nishimura M, Hara-Nishimura I. J. Biol. Chem. 2003; 278:33194. [PubMed: 12775715]

(7). Matthews SP, Werber I, Deussing J, Peters C, Reinheckel T, Watts C. J. Immunol. 2010; 184:2423. [PubMed: 20164435]

(8). Watts C. Nat. Immunol. 2004; 5:685. [PubMed: 15224094]

(9). Manoury B, Mazzeo D, Li DN, Billson J, Loak K, Benaroch P, Watts C. Immunity. 2003; 18:489. [PubMed: 12705852]

(10). Mattock KL, Gough PJ, Humphries J, Burnand K, Patel L, Suckling KE, Cuello F, Watts C, Gautel M, Avkiran M, Smith A. Atherosclerosis. 2010; 208:83. [PubMed: 19671471]

(11). Clerin V, Shih HH, Deng N, Hebert G, Resmini C, Shields KM, Feldman JL, Winkler A, Albert L, Maganti V, Wong A, Paulsen JE, Keith JC Jr. Vlasuk GP, Pittman DD. Atherosclerosis. 2008; 201:53. [PubMed: 18377911]

(12). Ishizaki T, Erickson A, Kuric E, Shamloo M, Hara-Nishimura I, Inacio AR, Wieloch T, Ruscher K. J. Cereb. Blood Flow Metab. 2010; 30:1756. [PubMed: 20234379]

(13). Gawenda J, Traub F, Luck HJ, Kreipe H, von Wasielewski R. Breast Cancer Res. Treat. 2007; 102:1. [PubMed: 17028987]

(14). Murthy RV, Arbman G, Gao J, Roodman GD, Sun XF. Clin. Cancer Res. 2005; 11:2293. [PubMed: 15788679]

(15). Wang L, Chen S, Zhang M, Li N, Chen Y, Su W, Liu Y, Lu D, Li S, Yang Y, Li Z, Stupack D, Qu P, Hu H, Xiang R. J. Cell. Biochem. 2012; 113:2679. [PubMed: 22441772]

(16). Wu W, Luo Y, Sun C, Liu Y, Kuo P, Varga J, Xiang R, Reisfeld R, Janda KD, Edgington TS, Liu C. Cancer Res. 2006; 66:970. [PubMed: 16424032]

(17). Luo Y, Zhou H, Krueger J, Kaplan C, Lee SH, Dolman C, Markowitz D, Wu W, Liu C, Reisfeld RA, Xiang R. J. Clin. Invest. 2006; 116:2132. [PubMed: 16862213]

(18). Hanahan D, Weinberg RA. Cell. 2011; 144:646. [PubMed: 21376230]

(19). Lewen S, Zhou H, Hu HD, Cheng T, Markowitz D, Reisfeld RA, Xiang R, Luo Y. Cancer Immunol. Immunother. 2008; 57:507. [PubMed: 17786443]

(20). Stern L, Perry R, Ofek P, Many A, Shabat D, Satchi-Fainaro R. Bioconjugate Chem. 2009; 20:500.

(21). Bajjuri KM, Liu Y, Liu C, Sinha SC. ChemMedChem. 2011; 6:54. [PubMed: 21154805]

(22). Lee J, Bogyo M. ACS Chem. Biol. 2010; 5:233. [PubMed: 20017516]

(23). Blum G, von Degenfeld G, Merchant MJ, Blau HM, Bogyo M. Nat. Chem. Biol. 2007; 3:668. [PubMed: 17828252]

(24). Blum G, Mullins SR, Keren K, Fonovic M, Jedeszko C, Rice MJ, Sloane BF, Bogyo M. Nat. Chem. Biol. 2005; 1:203. [PubMed: 16408036]

(25). Kato D, Boatright KM, Berger AB, Nazif T, Blum G, Ryan C, Chehade KA, Salvesen GS, Bogyo M. Nat. Chem. Biol. 2005; 1:33. [PubMed: 16407991]

(26). Sexton KB, Witte MD, Blum G, Bogyo M. Bioorg. Med. Chem. Lett. 2007; 17:649. [PubMed: 17189693]

(27). Loak K, Li DN, Manoury B, Billson J, Morton F, Hewitt E, Watts C. Biol. Chem. 2003; 384:1239. [PubMed: 12974392]

(28). Edgington LE, Berger AB, Blum G, Albrow VE, Paulick MG, Lineberry N, Bogyo M. Nat. Med. 2009; 15:967. [PubMed: 19597506]

(29). Adams C, Totpal K, Lawrence D, Marsters S, Pitti R, Yee S, Ross S, Deforge L, Koeppen H, Sagolla M, Compaan D, Lowman H, Hymowitz S, Ashkenazi A. Cell Death Differ. 2008; 15:751. [PubMed: 18219321]

(30). Edgington LE, van Raam BJ, Verdoes M, Wierschem C, Salvesen GS, Bogyo M. Chem. Biol. 2012; 19:340. [PubMed: 22444589]

(31). Li DN, Matthews SP, Antoniou AN, Mazzeo D, Watts C. J. Biol. Chem. 2003; 278:38980. [PubMed: 12860980]

(32). Xu Y, Schnorrer P, Proietto A, Kowalski G, Febbraio MA, Acha-Orbea H, Dickins RA, Villadangos JA. J. Immunol. 2011; 186:3666. [PubMed: 21300820]

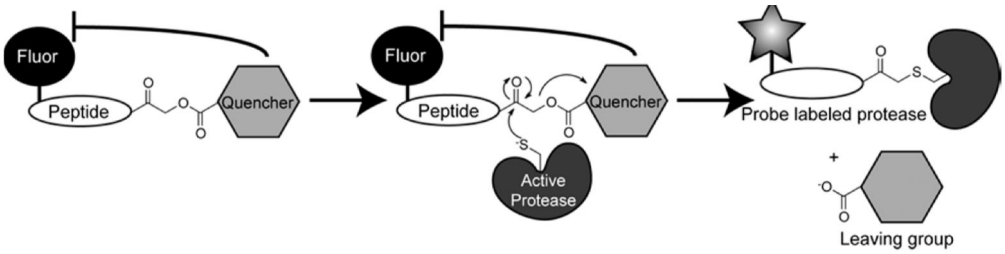

Figure 1.

Schematic of a quenched probe binding to a cysteine protease. Thiol attack of the acyloxymethyl ketone results in loss of the quenching group, leading to an increase in fluorescence emission.

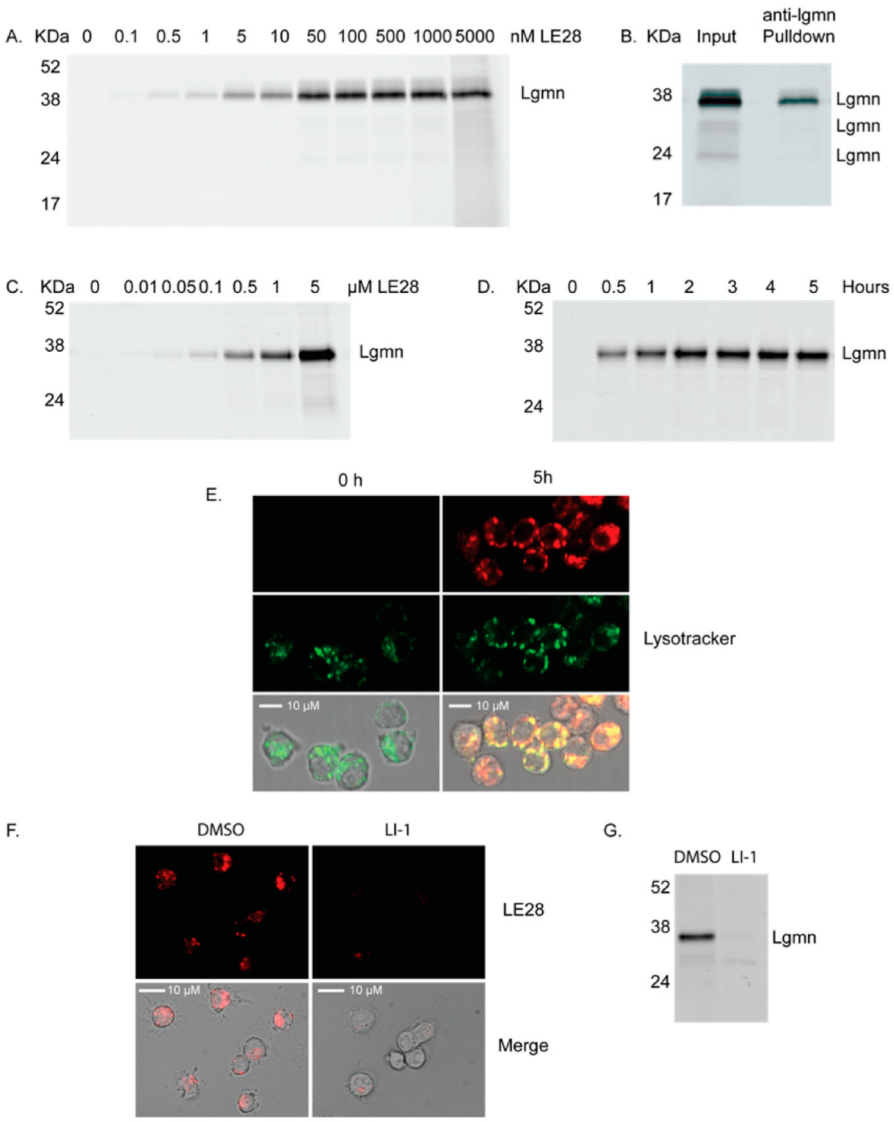

Figure 2.

(A) Fluorescent SDS-PAGE showing dose-dependent labeling of legumain by LE28 in RAW cell macrophage extracts. (B) Immunoprecipitation of LE28-labeled RAW cell lysates using a legumain-specific polyclonal antibody. (C) RAW cells were labeled at the indicated dose of LE28 for one hour followed by lysis and fluorescent SDS-PAGE. (D) RAW cells were incubated with 1 μM LE28 for the indicated time period followed by lysis and fluorescent SDS-PAGE. (E) Microscopy images of RAW cells exposed to LE28 (red) for 0 or 5 h. Lysotracker (green) was used to reveal the location of lysosomes. (F) Microscopy of RAW cells exposed to DMSO vehicle or 100 μM of the legumain inhibitor, LI-1 followed by incubation with LE28. (G) SDS-PAGE analysis of RAW cells exposed to DMSO vehicle or LI-1, followed by labeling with LE28.

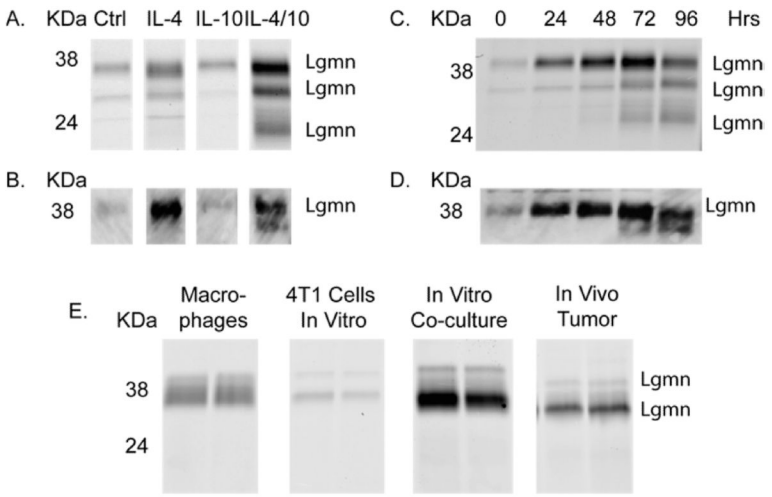

Figure 3.

Regulation of legumain activity. (A) Legumain activity in primary macrophages stimulated with the indicated cytokine, followed by labeling of intact cells by LE28 and fluorescent SDS-PAGE. (B) Antilegumain Western blot of samples in (A). (C) Time course of legumain activation in primary macrophages exposed to IL-4/-10. Intact cells were labeled with LE28 followed by SDS-PAGE. (D) Antilegumain Western blot of samples in (C). (E) Legumain activity in macrophages alone, in 4T1 tumor cells alone, or in coculture. The rightmost column shows activity in tumor cells that were implanted subcutaneously in mice for one week. For each group, lysates were prepared and labeled with LE28.

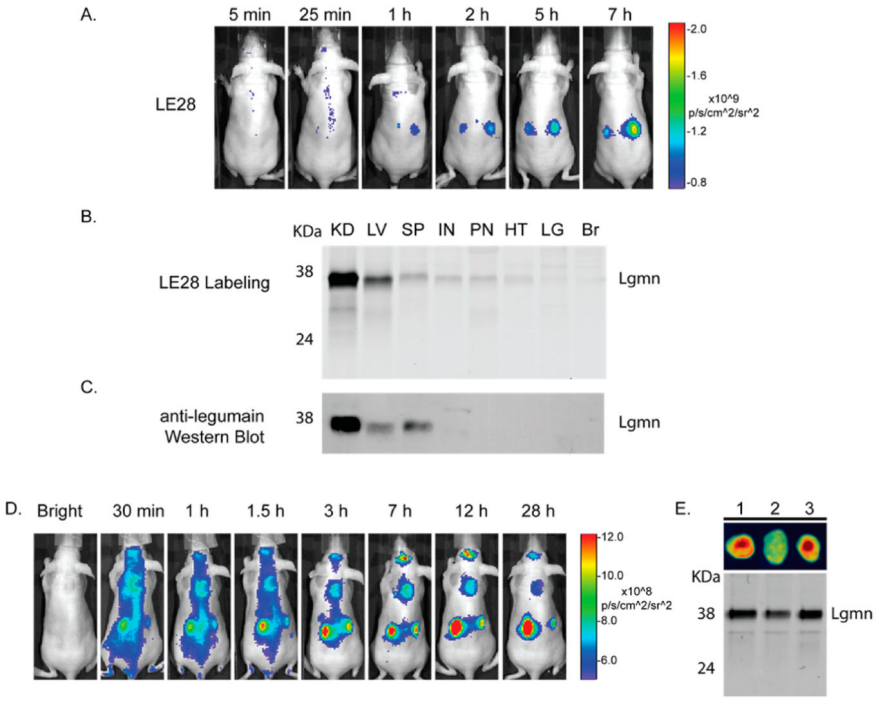

Figure 4.

In vivo imaging with LE28. (A) Clearance of the LE28 signal in normal mice imaged on an IVIS 100 machine. (B) Fluorescent SDS-PAGE analysis of tissues removed from mice after the indicated time and corresponding antilegumain Western blot. KD = kidney, LV = liver, SP = spleen, IN = intestine, PN = pancreas, HT = heart, LG = lung, and BR = brain. (C) Western blot analysis of total legumain expression in samples from (B) using a legumain-specific polyclonal antibody. (D) Mice bearing HCT-116 xenograft tumors on their backs were injected with LE28 and imaged over time using an IVIS 100. (E) Tumors from three mice were removed and imaged ex vivo, followed by fluorescent SDS-PAGE analysis.

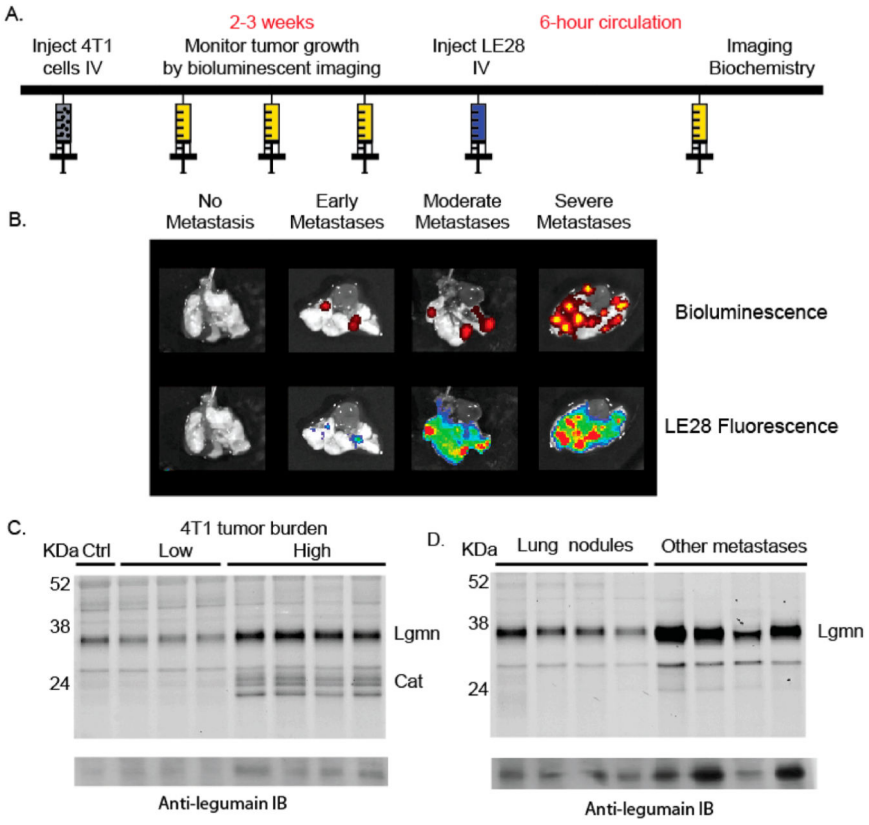

Figure 5.

Imaging legumain activity in a syngeneic tumor model. (A) Schematic of experimental setup. (B) Lungs bearing increasing burden of 4T1 experimental metastases were imaged for luciferase activity (bioluminescence) and legumain activity (LE28 fluorescence). (C) Whole lung lysates from (B) were analyzed by fluorescent SDS-PAGE and Western blot using a legumain-specific antobody. (D) Individual lung tumors from (B) were dissected as well as solid tumors arising in other regions of the peritoneum and analyzed by fluorescent SDS-PAGE and Western blot using a legumain-specific antobody.

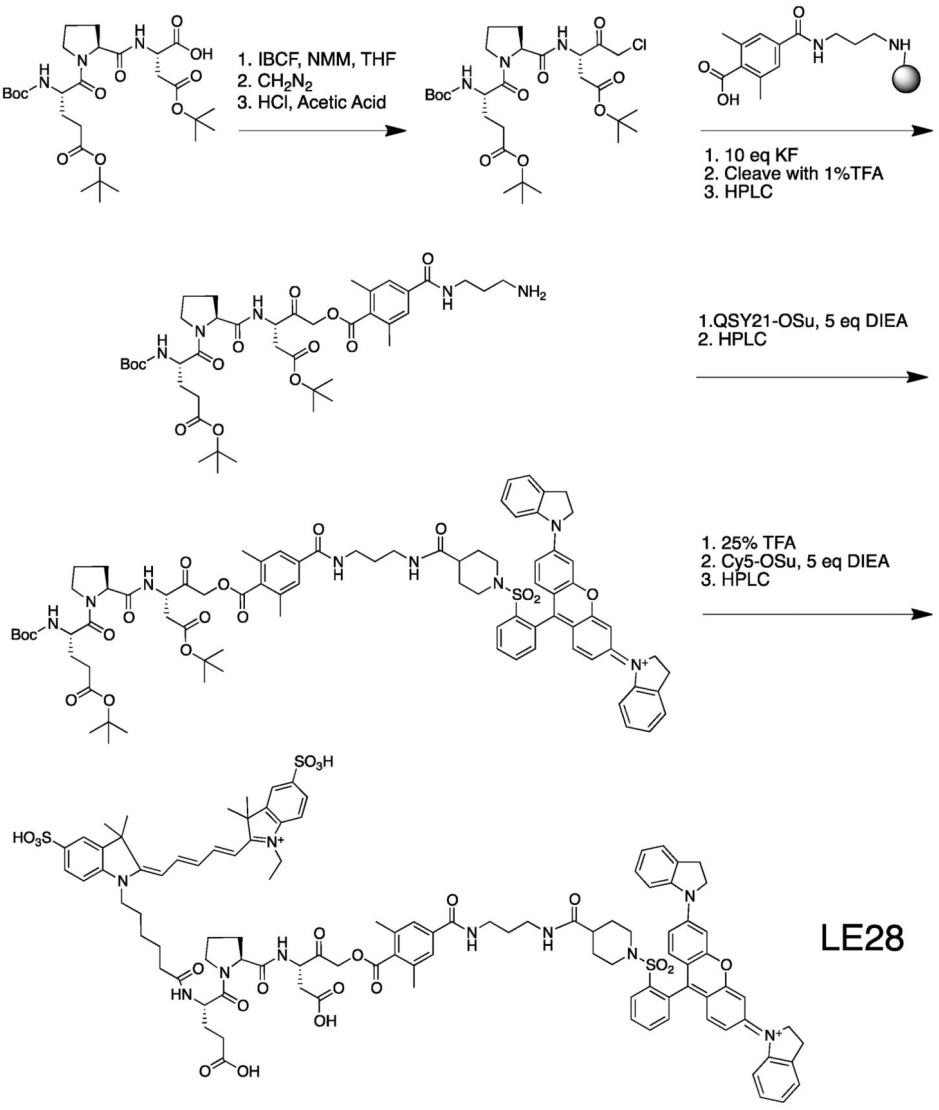

Scheme 1. Synthesis of LE28